HHS Public Access

Author manuscript

Nat Genet. Author manuscript; available in PMC 2015 April 01.

Published in final edited form as:

Nat Genet. 2014 October ; 46(10): 1120–1125. doi:10.1038/ng.3079.

Common variants near *ABCA1, AFAP1* and *GMDS* confer risk of primary open-angle glaucoma

Puya Gharahkhani[#1], **Kathryn P Burdon**[#2,3], **Rhys Fogarty**[2], **Shiwani Sharma**[2], **Alex W. Hewitt**[4], **Sarah Martin**[2], **Matthew H. Law**[1], **Katie Cremin**[5], **Jessica N. Cooke Bailey**[6,7], **Stephanie J. Loomis**[8], **Louis R. Pasquale**[8,9], **Jonathan L. Haines**[6,7], **Michael A. Hauser**[10,11], **Ananth C. Viswanathan**[12], **Peter McGuffin**[13], **Fotis Topouzis**[14], **Paul J. Foster**[12], **Stuart L Graham**[15], **Robert J Casson**[16], **Mark Chehade**[16], **Andrew J White**[17], **Tiger Zhou**[2], **Emmanuelle Souzeau**[2], **John Landers**[2], **Jude T Fitzgerald**[2], **Sonja Klebe**[18], **Jonathan B Ruddle**[4], **Ivan Goldberg**[19], **Paul R Healey**[17], **Wellcome Trust Case Control Consortium 2, NEIGHBORHOOD consortium**, **Richard A. Mills**[2], **Jie Jin Wang**[17], **Grant W. Montgomery**[1], **Nicholas G. Martin**[1], **Graham RadfordSmith**[1,20], **David C. Whiteman**[1], **Matthew A. Brown**[5], **Janey L. Wiggs**[8], **David A Mackey**[3,21], **Paul Mitchell**[17], **Stuart MacGregor**[1,*], and **Jamie E. Craig**[2,22,*]

[1] QIMR Berghofer Medical Research Institute, Brisbane, QLD 4029, Australia

[2] Department of Ophthalmology, Flinders University, Adelaide, SA 5042, Australia

[3] Menzies Research Institute Tasmania, University of Tasmania, Hobart, TAS, 7000, Australia

[4] Centre for Eye Research Australia (CERA), University of Melbourne, Royal Victorian Eye and Ear Hospital, Melbourne, Victoria, Australia

[5] University of Queensland Diamantina Institute, Brisbane, QLD 4102, Australia

[6] Center for Human Genetics Research, Vanderbilt University Medical Center, Nashville, Tennessee, USA

Corresponding author Correspondence should be addressed to Jamie Craig (jamie.craig@flinders.edu.au) or Puya Gharahkhani (Puya.Gharahkhani@qimrberghofer.edu.au)..

*These authors jointly directed this work.

URLs. PLINK, http://pngu.mgh.harvard.edu/~purcell/plink; R Project, http://www.r-project.org; LocusZoom, http://csg.sph.umich.edu/locuszoom; Ensembl, http://www.ensembl.org/index.html; NCBI, http://www.ncbi.nlm.nih.gov; UCSC genome Bioinformatics, http://genome.ucsc.edu; Genecards, http://www.genecards.org; UniprotKB, http://www.uniprot.org; ENCODE project, http://www.genome.gov/10005107; RegulomeDB, http://regulome.stanford.edu; HaploReg v2, http://www.broadinstitute.org/mammals/haploreg/haploreg.php; Genevar, http://www.sanger.ac.uk/resources/software/genevar.

AUTHOR CONTRIBUTIONS

K.P.B., S.MacGregor, and J.E.C. were involved in designing the study. A.W.H., K.C., L.R.P., M.A.H., A.C.V., P.MG., F.T., P.J.F., J.J.W., G.W.M., N.G.M., G.RS., D.C.W., M.A.B., J.L.W., D.A.M., P.M. and J.E.C. were involved in participant recruitment, sample collection or genotyping. Analysis was performed by P.G., R.F., K.P.B., S.S., M.H.L., J.N.C.B., S.J.L., L.R.P., J.L.H., J.L.W., and S.MacGregor. Designing and conducting the laboratory experiments were performed by K.P.B., S.S., S.M., and R.F. Clinician assessments were performed by S.L.G., R.J.C., M.C., A.J.W., T.Z., E.S., J.L., J.T.F., S.K., J.B.R., I.G., P.R.H., R.M., D.A.M. and J.E.C. The initial draft was written by P.G., K.P.B., S.S., and S.MacGregor.

COMPETING FINANCIAL INTERESTS

The authors declare no competing financial interests.

[7] Department of Epidemiology and Biostatistics, Case Western Reserve University, Cleveland, Ohio, USA

[8] Department of Ophthalmology, Harvard Medical School and Massachusetts Eye and Ear Infirmary, Boston, Massachusetts, USA

[9] Channing Division of Network Medicine, Brigham and Women's Hospital, Boston, Massachusetts, USA

[10] Department of Ophthalmology, Duke University Medical Center, Durham, North Carolina, USA

[11] Department of Medicine, Duke University Medical Center, Durham, North Carolina, USA

[12] NIHR Biomedical Research Centre, Moorfields Eye Hospital NHS Foundation Trust and UCL Institute of Ophthalmology, London, UK

[13] MRC Social Genetic and Developmental Psychiatry Research Centre, Institute of Psychiatry, King's College, De Crespigny Park, London, UK

[14] Department of Ophthalmology, School of Medicine, Aristotle University of Thessaloniki, AHEPA Hospital, Thessaloniki, Greece

[15] Ophthalmology and Vision Science, Macquarie University, Sydney, New South Wales, Australia

[16] South Australian Institute of Ophthalmology, University of Adelaide, Adelaide, South Australia, Australia

[17] Centre for Vision Research, Westmead Millennium Institute, University of Sydney, Westmead, NSW 2145, Australia

[18] Department of Anatomical Pathology, Flinders University, Flinders Medical Centre, South Australia

[19] Department of Ophthalmology, University of Sydney, Sydney Eye Hospital, Sydney, Australia

[20] School of Medicine, University of Queensland, Herston Campus, Brisbane, QLD, Australia

[21] Centre for Ophthalmology and Visual Science, Lions Eye Institute, University of Western Australia, Perth, Australia

[22] South Australian Health and Medical Research Institute, Adelaide, South Australia

[#] These authors contributed equally to this work.

Abstract

Primary open-angle glaucoma (POAG) is a major cause of irreversible blindness worldwide. We performed a genome-wide association study in an Australian discovery cohort comprising 1,155 advanced POAG cases and 1,992 controls. Association of the top SNPs from the discovery stage was investigated in two Australian replication cohorts (total 932 cases, 6,862 controls) and two US replication cohorts (total 2,616 cases, 2,634 controls). Meta-analysis of all cohorts revealed three novel loci associated with development of POAG. These loci are located upstream of *ABCA1* (rs2472493 [G] OR=1.31, $P = 2.1 \times 10^{-19}$), within *AFAP1* (rs4619890 [G] OR=1.20, $P = 7.0 \times 10^{-10}$) and within *GMDS* (rs11969985 [G] OR=1.31, and $P = 7.7 \times 10^{-10}$). Using RT-PCR and

immunolabelling, we also showed that these genes are expressed within human retina, optic nerve and trabecular meshwork and that ABCA1 and AFAP1 are also expressed in retinal ganglion cells.

POAG, the most common subtype of glaucoma, is characterised by a progressive loss of peripheral vision but patients may remain undiagnosed until central vision is affected[1,2]. POAG etiology and pathogenesis are poorly understood. Linkage, candidate gene and genome-wide association studies (GWAS) have identified several loci reproducibly associated with development of POAG[3-7]. Our previous GWAS of advanced POAG identified two loci at *TMCO1* and *CDKN2B-AS1*[6], with studies of non-advanced POAG also implicating *CAV1*[5], *SIX6* and a region on 8q22[7]. Here we use a three-stage GWAS to identify additional genetic loci associated with POAG in participants of European descent.

The stage 1 discovery cohort comprised 1,155 advanced glaucoma cases from the Australian & New Zealand Registry of Advanced Glaucoma (ANZRAG), and 1,992 controls, genotyped on Illumina Omni1M or OmniExpress arrays (Supplementary Notes, Supplementary Table 1). The genotype data from cases and controls were combined and cleaned, and 569,249 SNPs were used as the base of imputation against 1000 Genomes Phase 1 European ethnicity dataset. 7,594,768 SNPs were successfully imputed with Minor Allele Frequency (MAF) >0.01 and imputation quality score >0.8. Association analysis was performed using an additive model adjusted for sex and 6 principal components. The *P*-values from the association analysis were corrected for the estimated genomic inflation factor lambda, 1.06 (quantile-quantile plot shown in Supplementary Figure 1).

The stage 1 association results across the genome are shown in Supplementary Figure 2, and the association results for all SNPs with $P<1\times10^{-7}$ are shown in Supplementary Table 2. Two previously unreported regions reached genome-wide significance ($P<5\times10^{-8}$) in the stage 1 discovery cohort, with a further novel region associated at close to genome-wide significance (Table 1). The top novel associated SNPs were rs2472493[G] upstream of the ATP-Binding Cassette, Sub-Family A, Member 1 (*ABCA1)* gene on chromosome 9 (OR=1.43 and $P=2.0\times10^{-10}$), rs11827818[G] close to Rho guanine nucleotide exchange factor 12 (ARHGEF12) gene (OR=1.52 and $P=9.2\times10^{-9}$) on chromosome 11, and rs114096562[A] in *GDP-mannose 4,6-dehydratase (GMDS)* gene (OR=1.55 and $P=7.0\times10^{-8}$) on chromosome 6. The regional association results for these three SNPs are shown in Figure 1. We also performed the analysis after removing controls affected by other diseases (Supplementary Notes) and found the effect sizes were similar (Supplementary Table 3).

Associations of top SNPs in the discovery cohort were then investigated in a stage 2 set comprising two Australian replication datasets (ANZRAG and Blue Mountains Eye Study [BMES] datasets, in total 932 cases, 6,862 controls, Supplementary Notes, Supplementary Table 1). All replication cohort participants were of European descent. To make maximum valid use of our cohorts, for replication we focused on SNPs directly genotyped on the Illumina Human610/670 arrays; proxy genotyped SNPs were used where imputed data was not available for replication cohorts (Online Methods).

Examining all autosomal SNPs with $P < 1\times10^{-4}$ in stage 1 (twenty four SNPs with the best *P*-values were used as the lead SNPs, Supplementary Table 4), four regions showed nominal evidence (P<0.05 for seven SNPs in/near *ABCA1*, *GMDS*, *ITIH1* and *AFAP1*) for replication in the ANZRAG replication samples (Supplementary Table 4). When stages 1 and 2 were combined, SNPs near *ABCA1* and in *AFAP1* exceeded genome-wide significance ($P<5\times10^{-8}$ for rs2472493 and rs4619890) with consistent effect sizes and direction of effects among the cohorts (Supplementary Table 4, Table 2).

In the stage 3 replication, the newly identified top SNPs from stage 2 were examined in data available from two additional replication cohorts (see Supplementary Notes, Supplementary Table 1): NEIGHBOR and MEEI (total 2,616 cases, 2,634 controls). We also performed a meta-analysis of the results for these SNPs between all cohorts (discovery and all four replication cohorts) using the effect sizes and their standard errors. In the meta-analysis results, SNPs in/near *ABCA1*, *AFAP1* and *GMDS* genes clearly reached genome-wide significance ($P<5\times10^{-8}$) (Table 2).

The top SNP within *ARHGEF12* gene (rs2276035) did not reach the significance level ($P<5\times10^{-8}$) in our standard meta-analysis (Table 2), primarily due to heterogeneity between stage 1 and stages 2/3. This heterogeneity could be explained by the difference in the glaucoma status in these cohorts, the “winner's curse” effect that leads to inflated OR estimates in GWAS, or due to chance. The top SNP within *ITIH1* (rs2710323) was not genome-wide significant in our meta-analysis (Table 2).

At each of the novel loci, the effect size is larger in the discovery cohort than in the replication cohorts (Table 2). The discovery cohort comprises only advanced POAG cases, whereas the replication cohorts contained POAG cases representing a range of disease severity. One cannot directly infer however that the true effect size is largest in advanced POAG. A “winner's curse” effect in the ANZRAG discovery cohort would inflate the OR estimates. Furthermore, there may have been greater diagnostic certainty in advanced POAG. To further investigate if the novel loci conferred higher risk in advanced compared with non-advanced POAG, we performed a sub-analysis on the ANZRAG replication cohort. We found no consistent difference between the ORs for the non-advanced (N=605) and advanced (N=220) POAG cases separately (Supplementary Table 5). This sub-analysis, together with the significant results in the replication cohorts taken alone, suggest that the novel loci in this study are associated with POAG in general (not only advanced POAG), indicating the generalizability of our findings.

Intraocular pressure (IOP) was not a criterion in the definition of POAG in this study, because POAG patients may have normal or elevated IOP[8]. Thus, the novel loci identified in this study are associated with POAG in general, regardless of IOP levels. However, we had peak IOP measures available for 1,039 of the 1,155 cases in the ANZRAG discovery cohort. 330 (31.8%) of the individuals had Normal Tension Glaucoma (NTG) (IOP<=21 mm Hg), and 709 (68.2%) had High Tension Glaucoma (HTG) (IOP>21 mm Hg). We investigated the association of the novel loci identified in this study with 330 NTG and 709 HTG cases versus 1,992 population controls in the discovery cohort (Supplementary Table 6). The direction and magnitude of effect of the risk alleles were similar for NTG, HTG, and all

POAG (Supplementary Table 6 and Table 2). However, the analysis for NTG and HTG was less powerful compared to POAG due to the smaller sample size of the subgroups.

None of our newly identified POAG loci overlap with the previously published loci associated with the POAG sub-phenotypes including IOP and vertical cup-disk ratio (VCDR)[9-11]. We also investigated the association of the novel loci identified in this study with peak measured IOP in 1,039 POAG cases with available data in the ANZRAG discovery cohort. The novel loci were not associated with peak IOP in the ANZRAG discovery cohort (Supplementary Table 7), although the *ABCA1* SNP showed a trend toward significance (P=0.0675, two-sided test). The *ABCA1* glaucoma risk increasing allele acts in the expected direction on IOP (allele increases IOP), resulting in a *P* of 0.034 if one conducts a one-sided test. Larger sample sizes and further meta-analysis of multiple studies will unambiguously determine if the novel loci in this study are associated with sub-phenotypes such as IOP.

We also investigated previously reported GWAS hits identified in other studies[5-7] in the meta-analysis of results between our discovery and replication cohorts (Supplementary Table 8). The *TMCO1*, *CDKN2B-AS1* and *SIX6* loci were clearly genome-wide significant ($P<5\times10^{-8}$) while *CAV1/CAV2* and the locus on chromosome 8 were associated with POAG but not at genome-wide significance level. (. SNP rs11669977 at *NTF4* was not associated with POAG.

We used ENCODE project data[12] and the Genevar database[13] (expression quantitative trait locus, eQTL, database) to predict the possible functional effects of the top SNPs identified in this study. The top SNP rs2472493 located upstream of the *ABCA1* gene is an eQTL in lymphoblastoid cell lines (Genevar database) and may alter the sequence of motifs for proteins such as FOXJ2 and SIX5 (HaploReg v2[14]). One of the SNPs in high linkage disequilibrium (LD, $r^2>0.8$) with the top SNP near *ABCA1* (rs2472494) alters the regulatory motif for binding of PAX6 (HaploReg v2). *PAX6* is an established master control gene in eye development[15]. A SNP (rs28495790) in high LD ($r^2>0.8$) with the best SNP in *AFAP1* gene (rs4619890) is likely to affect binding of proteins (score 2b in RegulomeDB[16]) such as CTCF and RAD21 in variety of cell lines including WERI-Rb-1 (retinoblastoma). rs28495790 alters the sequence of regulatory motifs for binding of several proteins including PAX6 (HaploReg v2). This may suggest a regulatory role of this SNP in gene expression in a similar pathway to that of rs2472494 near *ABCA1* gene. In *GMDS*, rs3046543 (in high LD, $r^2=0.8$, with top imputed SNP rs114096562) alters the sequence of the regulatory motif for binding of SIX6; *SIX6* variants confer glaucoma risk[7]. SNPs close to *SIX6* also clearly reached genome-wide significance in the meta-analysis in this study (top SNP rs10483727[T] OR=1.32; $P=1.56\times10^{-17}$). These data suggest that the top SNPs identified in this study may have important regulatory roles.

ABCA1 is a membrane-bound receptor involved in phospholipid and cholesterol efflux from cells. *ABCA1* is expressed in retinal ganglion cells in monkey retina[17]; the cells that undergo apoptosis in glaucoma. We analysed expression of *ABCA1* mRNA in human ocular tissues by RT-PCR and found that the iris, ciliary body, retina, optic nerve head, optic nerve and trabecular meshwork cell lines derived from normal and glaucomatous eyes express the

main transcript that encodes the full-length protein (Supplementary Figure 3a). We also detected an alternative transcript in the ocular tissues (Supplementary Figure 3a) with unknown function[18,19]. Immunolabelling of sections of normal human eye with the anti-ABCA1 specific antibody (Supplementary Figure 4) showed distribution of the protein in the trabecular meshwork, all layers of the retina (including retinal ganglion cells), and the optic nerve (Figure 2). Similar ABCA1 labelling was observed in a glaucomatous eye including in the layers of the retina (Figure 2g). *ABCA1* has been reported to regulate neuroinflammation and neurodegeneration through co-ordinated activity in various cell types in mouse brain[20] and it may be involved in glaucoma through a similar function in the retina.

AFAP1 encodes a protein that binds to actin filaments and allows their crosslinking[21,22]. Actin cytoskeleton-modulating signals have been shown to be involved in the regulation of aqueous outflow and intraocular pressure[23-25], which are important parts of glaucoma pathogenesis. *AFAP1* encodes two isoforms, the neuronal cell-specific A isoform and the ubiquitously expressed B isoform. By RT-PCR, we detected expression of both the A and B isoforms, in human retina (Supplementary Figure 3c) and expression of the B isoform in other ocular tissues including iris, ciliary body, lens, optic nerve and optic nerve head, and in cultured trabecular meshwork cells (Supplementary Figure 3b). Consistent with the mRNA expression data, in normal human eye, AFAP1 positive immunolabelling was observed in the trabecular meshwork, retina (including retinal ganglion cells), and optic nerve (Supplementary Figure 5) using AFAP1-specific antibody (Supplementary Fig. 6). Similar AFAP1 labelling was observed in a glaucomatous eye including in the retina (Supplementary Figure 5g and 5h). These data indicate that AFAP1 function in the trabecular meshwork and retina may be relevant in glaucoma pathogenesis.

GMDS encodes a protein that is required for the first step in *de novo* synthesis of fucose[26]. Fucose is required for diverse biological functions such as growth factor receptor signalling[27]. Several studies have suggested the effects of growth factors on development of glaucoma[23,28-32]. *GMDS* expresses two variant transcripts, 1 and 2. We detected expression of the variant 1 transcript in human ocular tissues and cultured trabecular meshwork cells by RT-PCR (Supplementary Figure 3d), which indicates ubiquitous expression of the gene in the eye.

In this study, we identified three novel risk loci for POAG and we suggested related candidate genes and pathways that might be involved in developing POAG. These new loci, in addition to the previously known risk loci, will improve risk profiling for glaucoma with better opportunities for management of high-risk individuals. At present many cases of glaucoma remaining undiagnosed until severe visual loss occurs; early detection and treatment can slow disease progression and prevent blindness[33]. Further dissection of these new POAG risk loci is likely to lead to insights into the etiology of this common, irreversible cause of blindness.

Online methods

Study design

In total 1,155 glaucoma cases and 1,992 controls, genotyped on Illumina Omni1M or OmniExpress arrays and imputed to the 1000 Genomes Phase 1 Europeans panel, were used as discovery cohort in this study to perform a genome-wide association study for Primary Open Angle Glaucoma (POAG) (stage 1). The association results for the top SNPs from the discovery cohort were replicated in stage 2 and then stage 3 replication cohorts. The cohort details, genotyping platforms for each cohort and diagnostic criteria are listed in the Supplementary Notes. In addition, we performed a meta-analysis for the top SNPs in the discovery and replication cohorts. In this method section we have described the methods used for imputation and statistical analysis for the discovery cohort. Methods used for each replication cohort are present in the Supplementary Notes.

Quality Control (QC)

The QC for the discovery cohort was performed in PLINK[34] by removing individuals with more than 3% missing genotypes, SNPs with call rate <97%, minor allele frequency (MAF) <0.01, and Hardy-Weinberg equilibrium P<0.0001 in controls and P<5e-10 in cases. We used the same QC protocol before merging the cases and controls in our discovery cohort to avoid mismatches between the merged datasets. Following merging, the genotypes for 569,249 SNPs common to the arrays were taken forward for analysis. Identity by descent was computed in PLINK based on autosomal markers, with one of each pair of individuals with relatedness of > 0.2 removed. Principal components were computed for all participants and reference samples of known northern European ancestry (1000G British, CEU, Finland participants) using smartpca package from EIGENSOFT software[35,36]. Participants with PC1 or PC2 values > 6 standard deviations from the known northern European ancestry group were excluded.

Imputation

Imputation was conducted using IMPUTE2[37] in 1Mb sections, with the 1000 Genomes Phase 1 [38] Europeans (March 2012 release) as the reference panel. Genotyped SNPs who were strand ambiguous (e.g. A/T, C/G) were dropped from the input genotype panel prior to imputation; given these are deliberately under-represented on Illumina arrays this has limited effects on ability to impute data but gives greater confidence in the imputation's quality. Imputation was performed with the recommended settings for IMPUTE2 including a 250kb buffer flanking imputation sections; and the effective size of the sampled population as 20,000[37]. Reference panel SNPs with a minor allele <0.001 in Europeans were not imputed. SNPs with imputation quality score (INFO) > 0.8 and MAF> 0.01 were carried forward for analysis.

Statistical analysis

Association testing on the imputed data was performed in SNPTEST[39,40] using additive model (-frequentist 1) and full dosage scores (-method expected) with sex and the first 6 principal components fitted as covariates. Genomic inflation factor lambda was calculated to

investigate the presence of population stratification and inflation. The *P*-values were corrected for genomic inflation factor lambda. Q-Q and Manhattan plots were created in R[41] . Regional association plots for the regions reaching genome-wide significance were created using LocusZoom[42] .

In order to investigate whether any hits identified in the discovery cohort were driven by a subset of controls affected by the other diseases (oesophageal cancer, Barrett's oesophagus, and inflammatory bowel diseases) we also performed a genome-wide association analysis after removing the controls who were affected by the other diseases (refer to the Supplementary Notes for the structure of controls in the discovery cohort). This analysis included 1,155 glaucoma cases and 1,147 controls.

Associations of top autosomal SNPs in the discovery cohort ($P < 1\times10^{-4}$) (stage 1) were investigated in the replication cohorts (stage 2 and 3) (refer to the Supplementary Notes for the structure of replication cohorts, QC and statistical analysis for each cohort). Stage 2 included two Australian replication data sets (total 932 cases, 6,862 controls) and stage 3 included two US cohorts (total 2,616 cases, 2,634 controls). For replication in stage 2, twenty four SNPs with the best *P*-values in the discovery cohort were used as the lead SNPs for the autosomal regions with $P < 1\times10^{-4}$ (Supplementary Table 4). The SNPs that were nominally replicated in stage 2 ($P<0.05$) were taken forward for replication in stage 3. To make maximum valid use of our cohorts, for replication we focused on SNPs directly genotyped on the Illumina Human610/670 arrays. Since a portion of the stage 2 cases were genotyped on a non-genomewide platform (Sequenom) we could not accurately evaluate the imputed SNPs from stage 1. Hence the most-associated SNP upstream of the *ABCA1* (rs2472493), and SNPs in high LD with the most-associated SNP near *ARHGEF12* (rs11217878 and rs2276035, $r^2=1$ and $r^2=0.94$, respectively with rs11827818) were used in the replication studies. Similarly, SNPs with high LD with the most-associated SNP in *GMDS* (rs2761233 and rs11969985, $r^2=0.93$ and $r^2=0.87$, respectively) with rs114096562, the most associated SNP in *GMDS*, were used for replication studies.

Fixed-effects meta-analysis for the top SNPs was performed between the discovery and replication cohorts in METAL[43] using the effect sizes and their standard errors for the risk alleles. Presence of heterogeneity between the cohorts for effect sizes of risk alleles was investigated using the I2 statistic, as implemented in METAL.

Identifying candidate genes

Candidate genes in the regions of association were selected based on the location and function of the genes, the pathways that the genes are involved in, tissue location of the expression of the gene, and whether similar phenotypes were reported to be caused by mutations in these genes. This information was found in Ensembl[44] , NCBI , UCSC genome Bioinformatics[45] , Genecards[46] , and UniprotKB[47] , as well as available published data. To predict functional effects of the top POAG associated SNPs identified in this study, we used the ENCODE project data[48] and the associated databases, RegulomeDB[49] and HaploReg v2[50] . We used Genevar database[51] to investigate expression quantitative trait loci within genetic regions of interest.

Expression analysis of genes at associated loci in ocular tissues and cells

Ocular tissues from post-mortem human eyes were obtained through the Eye Bank of South Australia, according to guidelines of the Southern Adelaide Clinical Human Research Ethics Committee. Normal and glaucomatous trabecular meshwork cell lines, NTM-5 and GTM-3, were a kind gift from Dr Clark Abbot, Alcon Research Ltd., USA. Both the cell lines tested negative for mycoplasma contamination. Total RNA was extracted using the RNeasy Mini Kit (Qiagen Pty Ltd., Doncaster, Australia). First strand cDNA was synthesised using the Superscript III reverse transcriptase (Invitrogen, Life Technologies Australia Pty Ltd., Mulgrave, Australia) and random hexamers. PCR was performed using the Hot Star Taq Plus polymerase (Qiagen) and gene-specific primers (Supplementary Table 9). PCR was performed at the conditions specified in Supplementary Table 9. The enzyme was activated at 95°C for 5 min, denaturation was at 95°C for 30 sec, and elongation at 72°C. Additional elongation at 72°C for 5 min was allowed after completion of the amplification cycles. Specificity of each amplified product was confirmed by sequencing.

Immunohistochemical labelling

Eye tissue was fixed in neutral buffered formalin and embedded in paraffin. For immunolabelling, 4 μm sections were blocked with 5% normal goat serum and incubated with the mouse anti-ABCA1 (1:2000, cat# Ab66217, Sapphire Biosciences, NSW, Australia) or anti-AFAP (1:1000, BD Transduction Laboratories, CA, USA, cat# 610200) primary antibody at 4°C overnight. Primary antibody binding was detected with the Novolink Polymer detection kit (Leica Microsystems, Bannockburn, IL, USA) and Chromogen substrate coloration (Dako, Glostrup, Denmark). Sections were counterstained with haematoxylin and mounted in dePeX (Merck KGaA, Darmstadt, Germany). Light microscopy was performed on Olympus BX50 brightfield upright microscope attached with a Q-Imaging colour CCD camera; images were taken using the QCapture software (Q-Imaging Corporate, Surry, BC, Canada).

Western blotting

For Western blotting, proteins from NTM-5 and GTM-3 human trabecular meshwork cells, respectively, established from a normal and an individual with glaucoma, were extracted in RIPA buffer, analysed by SDS-PAGE using the mini-PROTEAN TGX gel and transferred onto PVDF membrane (Bio-Rad Laboratories Pty. Ltd., NSW, Australia). Western blotting was performed using the mouse anti-ABCA1 (1:500, cat# Ab66217, Sapphire Biosciences, NSW, Australia) or anti-AFAP (1:250, BD Transduction Laboratories, CA, USA, cat# 610200) primary antibody followed by hybridisation with the hydrogen peroxide conjugated goat anti-mouse IgG secondary antibody (1:1000, Jackson ImmunoResearch Laboratories Inc., Brisbane, Australia, cat# 115-035-003). ABCA1 antibody binding was detected using the Pierce SuperSignal West Pico (Jackson ImmunoResearch Laboratories Inc., Brisbane, Australia) and AFAP1 antibody binding using ECL Prime (GE Healthcare Australia and New Zealand, Sydney, Australia), chemiluminescence reagents.

Supplementary Material

Refer to Web version on PubMed Central for supplementary material.

Acknowledgements

Australian & New Zealand Registry of Advanced Glaucoma (ANZRAG)

Support for recruitment of ANZRAG was provided by the Royal Australian and New Zealand College of Ophthalmology (RANZCO) Eye Foundation. Genotyping was funded by the National Health and Medical Research Council of Australia (#535074 and #1023911). This work was also supported by funding from NHMRC #1031362 awarded to J.E.C., NHMRC #1037838 awarded to A.W.H., NHMRC #1048037 awarded to S.L.G., NHMRC #1009844 awarded to R.J.C. and I.G., NHMRC #1031920 and Alcon Research Institute grant awarded to D.A.M., Allergan Unrestricted grant awarded to A.J.W., and the BrightFocus Foundation and a Ramaciotti Establishment Grant. The authors acknowledge the support of Ms Bronwyn Usher-Ridge in patient recruitment and data collection, and Dr Patrick Danoy and Dr Johanna Hadler for genotyping.

Controls for the *ANZRAG* discovery cohort were drawn from the Australian Cancer Study, the Study of Digestive Health, and from a study of inflammatory bowel diseases. The Australian Cancer Study was supported by the Queensland Cancer Fund and the National Health and Medical Research Council (NHMRC) of Australia (Program no. 199600, awarded to David C. Whiteman, Adele C. Green, Nicholas K. Hayward, Peter G. Parsons, David M. Purdie, and Penelope M. Webb; and program no. 552429 awarded to David C. Whiteman). The Study of Digestive Health was supported by grant number 5 R01 CA 001833 from the US National Cancer Institute (awarded to David C. Whiteman).

The Barrett's and Esophageal Adenocarcinoma Genetic Susceptibility Study (BEAGESS) sponsored the genotyping of oesophageal cancer and Barrett's oesophagus cases, which were used as unscreened controls in the *ANZRAG* discovery cohort. BEAGESS was funded by grant R01 CA136725 from the US National Cancer Institute.

Genotyping for part of the Australian twin control sample included in the *ANZRAG* replication cohort was funded by an NHMRC Medical Genomics Grant. Genotyping for the remainder of twin controls was performed by the National Institutes of Health (NIH) Center for Inherited Research (CIDR) as part of an NIH/National Eye Institute (NEI) grant 1RO1EY018246, and we are grateful to Dr Camilla Day and staff. We acknowledge with appreciation all women who participated in the QIMR endometriosis study. We thank Endometriosis Associations for supporting study recruitment. We thank Sullivan Nicolaides and Queensland Medical Laboratory for pro bono collection and delivery of blood samples and other pathology services for assistance with blood collection. The QIMR twin and endometriosis studies were supported by grants from the National Health and Medical Research Council (NHMRC) of Australia (241944, 339462, 389927,389875, 389891, 389892, 389938, 443036, 442915, 442981, 496610, 496739, 552485, 552498), the Cooperative Research Centre for Discovery of Genes for Common Human Diseases (CRC), Cerylid Biosciences (Melbourne), and donations from Neville and Shirley Hawkins. We thank Margaret J. Wright, Megan J. Campbell, Anthony Caracella, Scott Gordon, Dale R Nyholt, Anjali K Henders, B. Haddon, D. Smyth, H. Beeby, O. Zheng, B. Chapman for their input into project management, databases, sample processing, and genotyping. We are grateful to the many research assistants and interviewers for assistance with the studies contributing to the QIMR twin collection.

Blue Mountains Eye Study (BMES)

BMES was supported by the Australian National Health & Medical Research Council (NH&MRC), Canberra Australia (974159, 211069, 457349, 512423, 475604, 529912); the Centre for Clinical Research Excellence in Translational Clinical Research in Eye Diseases; NH&MRC Senior Research Fellowships (358702, 632909 to J.J. Wang); and the Wellcome Trust, UK as part of Wellcome Trust Case Control Consortium 2 (A. Viswanathan, P. McGuffin, P. Mitchell, F. Topouzis, P. Foster) for genotyping costs of the entire BMES population (085475B08Z, 08547508Z, 076113). P.J.F. is also supported by the Medical Research Council (MRC) - G0401527, Research Into Ageing (Ref 262), and NIHR (UK) Biomedical Research Centre at Moorfields Eye Hospital and UCL Institute of Ophthalmology (BRC2_009) funds.

The BMES acknowledges Elena Rochtchina from the Centre for Vision Research, Department of Ophthalmology and Westmead Millennium Institute University of Sydney (NSW Australia); John Attia, Rodney Scott, Elizabeth G. Holliday from the University of Newcastle (Newcastle, NSW Australia); Jing Xie and Paul N. Baird from the Centre for Eye Research Australia, University of Melbourne; Michael T. Inouye, Medical Systems Biology, Department of Pathology & Department of Microbiology & Immunology, University of Melbourne (Victoria, Australia); Xueling Sim, National University of Singapore.

National Eye Institute (NEI) Glaucoma Human Genetics Collaboration (NEIGHBOR)

Genotyping services for the NEIGHBOR study were provided by the Center for Inherited Disease Research (CIDR) and were supported by the National Eye Institute through grant HG005259-01 (JL Wiggs). Additionally, CIDR is funded through a federal contract from the National Institutes of Health to The Johns Hopkins University, contract number HHSN268200782096C. Collecting and processing samples for the NEIGHBOR dataset was supported by

the National Eye Institute through ARRA grants 3R01EY015872-05S1 (JL Wiggs) and 3R01EY019126-02S1 (MA Hauser). Genotype imputation and meta-analysis were supported by EY022305 (JL Wiggs). Funding for the collection of cases and controls was provided by NIH grants: EY015543 (RR Allingham), EY006827 (D Gaasterland); HL73042, HL073389, EY13315, EY023646 (MA Hauser); CA87969 (JH Kang), CA49449 (JH Kang), CA55075 (JH Kang), EY009149 (PR Lichter), HG004608 (C McCarty), EY008208 (FA Medeiros), EY015473 (LR Pasquale), EY012118 (M Pericak-Vance), EY015682 (A Realini), EY011671 (JE Richards), EY09580 (JE Richards), EY013178 (JS Schuman), RR015574, EY015872 (JL Wiggs), EY010886 (JL Wiggs), EY009847 (JL Wiggs), EY014104 (JL Wiggs), EY011008, EY144428 (K Zhang), EY144448 (K Zhang), EY18660 (K Zhang). JL Wiggs and LR Pasquale are also supported by the Harvard Glaucoma Center for Excellence and the Margolis Fund. Y Liu is supported by the Glaucoma Research Foundation, American Health Assistance Foundation, and the Glaucoma Foundation. JL Wiggs, LR Pasquale, DC Musch, and JE Richards are supported by Research to Prevent Blindness. JN Cooke Bailey is supported by NIH T32 EY007157 (CWRU) and T32 EY21453-2 (VUMC).

MEEI case control sample:

Genotyping for the Massachusetts Eye and Ear Infirmary (MEEI) case control sample was performed at the Broad Institute of MIT and Harvard with funding support from the NIH GEI (Gene environment initiative) (U01HG04424 and U01HG004728). The GENEVA Coordinating Center (U01HG004446) assisted with genotype cleaning. Imputation was supported by NIH EY022305. Collection of cases and controls was supported by NIH EY015872.

Support for molecular analysis of the associated genes was provided by the Ophthalmic Research Institute of Australia. The authors acknowledge the support of Ms Margaret Philpott in collection of cadaveric human eye tissues, and Dr Nicholas Mabarrack for initial optimisation of the anti-AFAP antibody.

S MacGregor is supported by Australian Research Council (ARC) and Australian National Health & Medical Research Council (NHMRC) Fellowships. GW Montgomery, MA Brown, KP Burdon, DC Whiteman, and JE Craig are supported by Australian NHMRC Fellowships. David C. Whiteman was funded by the ARC and G. Radford-Smith by NHMRC during the period of this study.

The authors would like to acknowledge C. Abbot (Alcon Research Ltd.) for providing normal and glaucomatous trabecular meshwork cell lines, NTM-5 and GTM-3, respectively, as a kind gift.

References

1. Quigley HA, Broman AT. The number of people with glaucoma worldwide in 2010 and 2020. Br J Ophthalmol. 2006; 90:262–7. [PubMed: 16488940]
2. Casson RJ, Chidlow G, Wood JP, Crowston JG, Goldberg I. Definition of glaucoma: clinical and experimental concepts. Clin Experiment Ophthalmol. 2012; 40:341–9. [PubMed: 22356435]
3. Stone EM, et al. Identification of a gene that causes primary open angle glaucoma. Science. 1997; 275:668–70. [PubMed: 9005853]
4. Pasutto F, et al. Heterozygous NTF4 mutations impairing neurotrophin-4 signaling in patients with primary open-angle glaucoma. Am J Hum Genet. 2009; 85:447–56. [PubMed: 19765683]
5. Thorleifsson G, et al. Common variants near CAV1 and CAV2 are associated with primary open-angle glaucoma. Nat Genet. 2010; 42:906–9. [PubMed: 20835238]
6. Burdon KP, et al. Genome-wide association study identifies susceptibility loci for open angle glaucoma at TMCO1 and CDKN2B-AS1. Nat Genet. 2011; 43:574–8. [PubMed: 21532571]
7. Wiggs JL, et al. Common variants at 9p21 and 8q22 are associated with increased susceptibility to optic nerve degeneration in glaucoma. PLoS Genet. 2012; 8:e1002654. [PubMed: 22570617]
8. Quigley HA. Open-angle glaucoma. N Engl J Med. 1993; 328:1097–106. [PubMed: 8455668]
9. Ozel AB, et al. Genome-wide association study and meta-analysis of intraocular pressure. Hum Genet. 2014; 133:41–57. [PubMed: 24002674]
10. van Koolwijk LM, et al. Common genetic determinants of intraocular pressure and primary open-angle glaucoma. PLoS Genet. 2012; 8:e1002611. [PubMed: 22570627]
11. Ramdas WD, et al. A genome-wide association study of optic disc parameters. PLoS Genet. 2010; 6:e1000978. [PubMed: 20548946]
12. ENCODE_Project_Consortium. A user's guide to the encyclopedia of DNA elements (ENCODE). PLoS Biol. 2011; 9:e1001046. [PubMed: 21526222]

13. Yang TP, et al. Genevar: a database and Java application for the analysis and visualization of SNP-gene associations in eQTL studies. Bioinformatics. 2010; 26:2474–6. [PubMed: 20702402]
14. Ward LD, Kellis M. HaploReg: a resource for exploring chromatin states, conservation, and regulatory motif alterations within sets of genetically linked variants. Nucleic Acids Res. 2012; 40:D930–4. [PubMed: 22064851]
15. Hanson IM, et al. PAX6 mutations in aniridia. Hum Mol Genet. 1993; 2:915–20. [PubMed: 8364574]
16. Boyle AP, et al. Annotation of functional variation in personal genomes using RegulomeDB. Genome Res. 2012; 22:1790–7. [PubMed: 22955989]
17. Tserentsoodol N, et al. Intraretinal lipid transport is dependent on high density lipoprotein-like particles and class B scavenger receptors. Mol Vis. 2006; 12:1319–33. [PubMed: 17110915]
18. Bellincampi L, et al. Identification of an alternative transcript of ABCA1 gene in different human cell types. Biochem Biophys Res Commun. 2001; 283:590–7. [PubMed: 11341765]
19. Singaraja RR, et al. Alternate transcripts expressed in response to diet reflect tissue-specific regulation of ABCA1. J Lipid Res. 2005; 46:2061–71. [PubMed: 16024915]
20. Karasinska JM, et al. ABCA1 influences neuroinflammation and neuronal death. Neurobiol Dis. 2013; 54:445–55. [PubMed: 23376685]
21. Qian Y, et al. PC phosphorylation increases the ability of AFAP-110 to cross-link actin filaments. Mol Biol Cell. 2002; 13:2311–22. [PubMed: 12134071]
22. Qian Y, Baisden JM, Zot HG, Van Winkle WB, Flynn DC. The carboxy terminus of AFAP-110 modulates direct interactions with actin filaments and regulates its ability to alter actin filament integrity and induce lamellipodia formation. Exp Cell Res. 2000; 255:102–13. [PubMed: 10666339]
23. Junglas B, et al. Connective tissue growth factor causes glaucoma by modifying the actin cytoskeleton of the trabecular meshwork. Am J Pathol. 2012; 180:2386–403. [PubMed: 22542845]
24. Kwon HS, Lee HS, Ji Y, Rubin JS, Tomarev SI. Myocilin is a modulator of Wnt signaling. Mol Cell Biol. 2009; 29:2139–54. [PubMed: 19188438]
25. Inoue T, Tanihara H. Rho-associated kinase inhibitors: a novel glaucoma therapy. Prog Retin Eye Res. 2013; 37:1–12. [PubMed: 23770081]
26. Becker DJ, Lowe JB. Fucose: biosynthesis and biological function in mammals. Glycobiology. 2003; 13:41R–53R.
27. Miyoshi E, Moriwaki K, Nakagawa T. Biological function of fucosylation in cancer biology. J Biochem. 2008; 143:725–9. [PubMed: 18218651]
28. Inatani M, et al. Transforming growth factor-beta 2 levels in aqueous humor of glaucomatous eyes. Graefes Arch Clin Exp Ophthalmol. 2001; 239:109–13. [PubMed: 11372538]
29. Picht G, Welge-Luessen U, Grehn F, Lutjen-Drecoll E. Transforming growth factor beta 2 levels in the aqueous humor in different types of glaucoma and the relation to filtering bleb development. Graefes Arch Clin Exp Ophthalmol. 2001; 239:199–207. [PubMed: 11405069]
30. Ozcan AA, Ozdemir N, Canataroglu A. The aqueous levels of TGF-beta2 in patients with glaucoma. Int Ophthalmol. 2004; 25:19–22. [PubMed: 15085971]
31. Pena J, Taylor A, Ricard C, Vidal I, Hernandez M. Transforming growth factor β isoforms in human optic nerve heads. Br J Ophthalmol. 1999; 83:209–218. [PubMed: 10396201]
32. Fleenor DL, et al. TGFbeta2-induced changes in human trabecular meshwork: implications for intraocular pressure. Invest Ophthalmol Vis Sci. 2006; 47:226–34. [PubMed: 16384967]
33. Heijl A, Leske MC, Bengtsson B, Hyman L, Hussein M. Reduction of intraocular pressure and glaucoma progression: results from the Early Manifest Glaucoma Trial. Arch Ophthalmol. 2002; 120:1268–79. [PubMed: 12365904]
34. Purcell S, et al. PLINK: a tool set for whole-genome association and population-based linkage analyses. Am J Hum Genet. 2007; 81:559–75. [PubMed: 17701901]
35. Patterson N, Price AL, Reich D. Population structure and eigenanalysis. PLoS Genet. 2006; 2:e190. [PubMed: 17194218]
36. Price AL, et al. Principal components analysis corrects for stratification in genome-wide association studies. Nat Genet. 2006; 38:904–9. [PubMed: 16862161]

37. Howie BN, Donnelly P, Marchini J. A flexible and accurate genotype imputation method for the next generation of genome-wide association studies. PLoS Genet. 2009; 5:e1000529. [PubMed: 19543373]
38. 1000_Genomes_Project_Consortium. A map of human genome variation from population-scale sequencing. Nature. 2010; 467:1061–73. [PubMed: 20981092]
39. Wellcome_Trust_Case_Control_Consortium. Genome-wide association study of 14,000 cases of seven common diseases and 3,000 shared controls. Nature. 2007; 447:661–78. [PubMed: 17554300]
40. Marchini J, Howie B. Genotype imputation for genome-wide association studies. Nat Rev Genet. 2010; 11:499–511. [PubMed: 20517342]
41. R Core Team. R: A Language and Environment for Statistical Computing. (Vienna, Austria). 2013
42. Pruim RJ, et al. LocusZoom: regional visualization of genome-wide association scan results. Bioinformatics. 2010; 26:2336–7. [PubMed: 20634204]
43. Willer CJ, Li Y, Abecasis GR. METAL: fast and efficient meta-analysis of genomewide association scans. Bioinformatics. 2010; 26:2190–1. [PubMed: 20616382]
44. Flicek P, et al. Ensembl 2014. Nucleic Acids Res. 2014; 42:D749–55. [PubMed: 24316576]
45. Kent WJ, et al. The human genome browser at UCSC. Genome Res. 2002; 12:996–1006. [PubMed: 12045153]
46. Safran M, et al. GeneCards Version 3: the human gene integrator. Database (Oxford). 20102010:baq020. [PubMed: 20689021]
47. UniProt_Consortium. Activities at the Universal Protein Resource (UniProt). Nucleic Acids Res. 2014; 42:D191–8. [PubMed: 24253303]
48. ENCODE_Project_Consortium. A user's guide to the encyclopedia of DNA elements (ENCODE). PLoS Biol. 2011; 9:e1001046. [PubMed: 21526222]
49. Boyle AP, et al. Annotation of functional variation in personal genomes using RegulomeDB. Genome Res. 2012; 22:1790–7. [PubMed: 22955989]
50. Ward LD, Kellis M. HaploReg: a resource for exploring chromatin states, conservation, and regulatory motif alterations within sets of genetically linked variants. Nucleic Acids Res. 2012; 40:D930–4. [PubMed: 22064851]
51. Yang TP, et al. Genevar: a database and Java application for the analysis and visualization of SNP-gene associations in eQTL studies. Bioinformatics. 2010; 26:2474–6. [PubMed: 20702402]

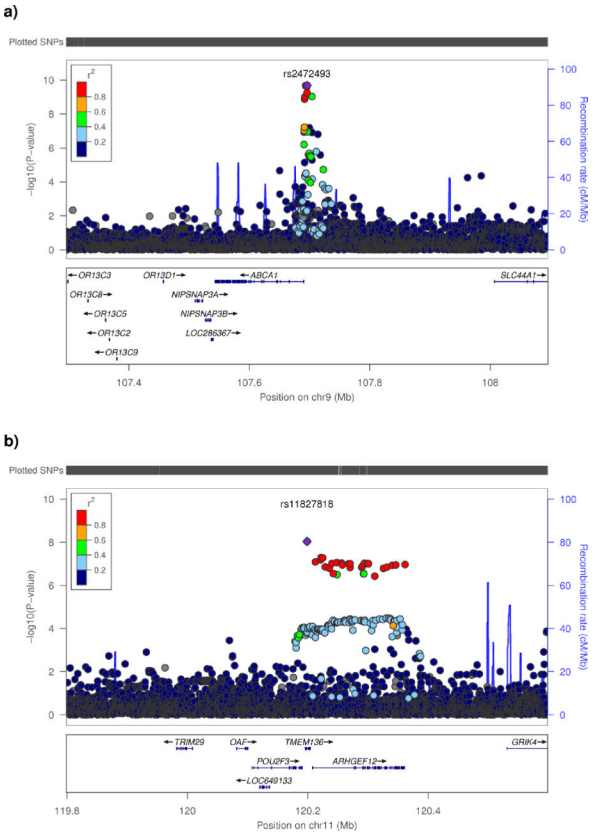

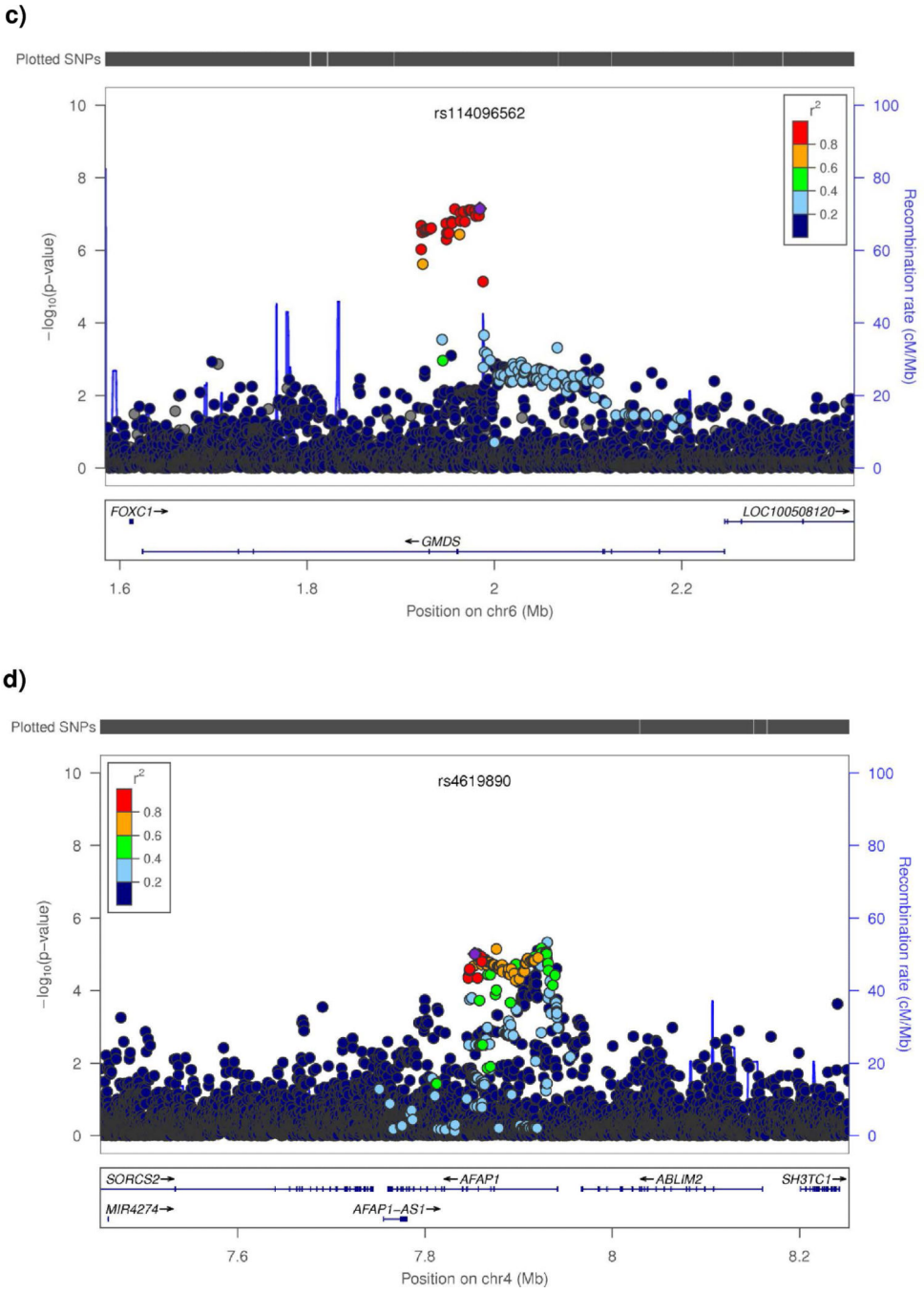

Figure 1. Association results for the regions reaching genome-wide significance

These plots show the regional association (using logistic regression with sex and the first 6 principal components fitted as covariates) and recombination rates for the top SNPs in the discovery dataset (1,155 advanced POAG cases and 1,992 controls). In each plot, the solid diamond indicates the top-ranked SNP in the region based on two-sided *P*-value. The colour box at the right or left corner of each plot indicates the pairwise correlation (R^2) between the top SNP and the other SNPs in the region. The blue spikes show the estimated recombination rates. The box underneath each plot shows the gene annotations in the region.

Each plot was created using LocusZoom (http://csg.sph.umich.edu/locuszoom/) for the top-ranked SNP in each region with 400-kb region surrounding it. (**a**) The top-ranked SNP for this plot is rs2472493 on chromosome 9 upstream of *ABCA1 gene* with $P=2.0\times10^{-10}$. (**b**) The top-ranked SNP for this plot is rs11827818 on chromosome 11 near *ARHGEF12* with $P = 9.2 \times 10^{-9}$. (**c**) The top-ranked SNP for this plot is rs114096562 on chromosome 6 in *GMDS* gene with $P=7.0\times10^{-8}$. (**d**) This plot is centred on rs4619890 SNP on chromosome 4 in *AFAP1* gene with $P=9.7\times10^{-6}$. This SNP clearly reached genome-wide significance ($P=7.0\times10^{-10}$) in the meta-analysis of the results between the discovery and replication cohorts.

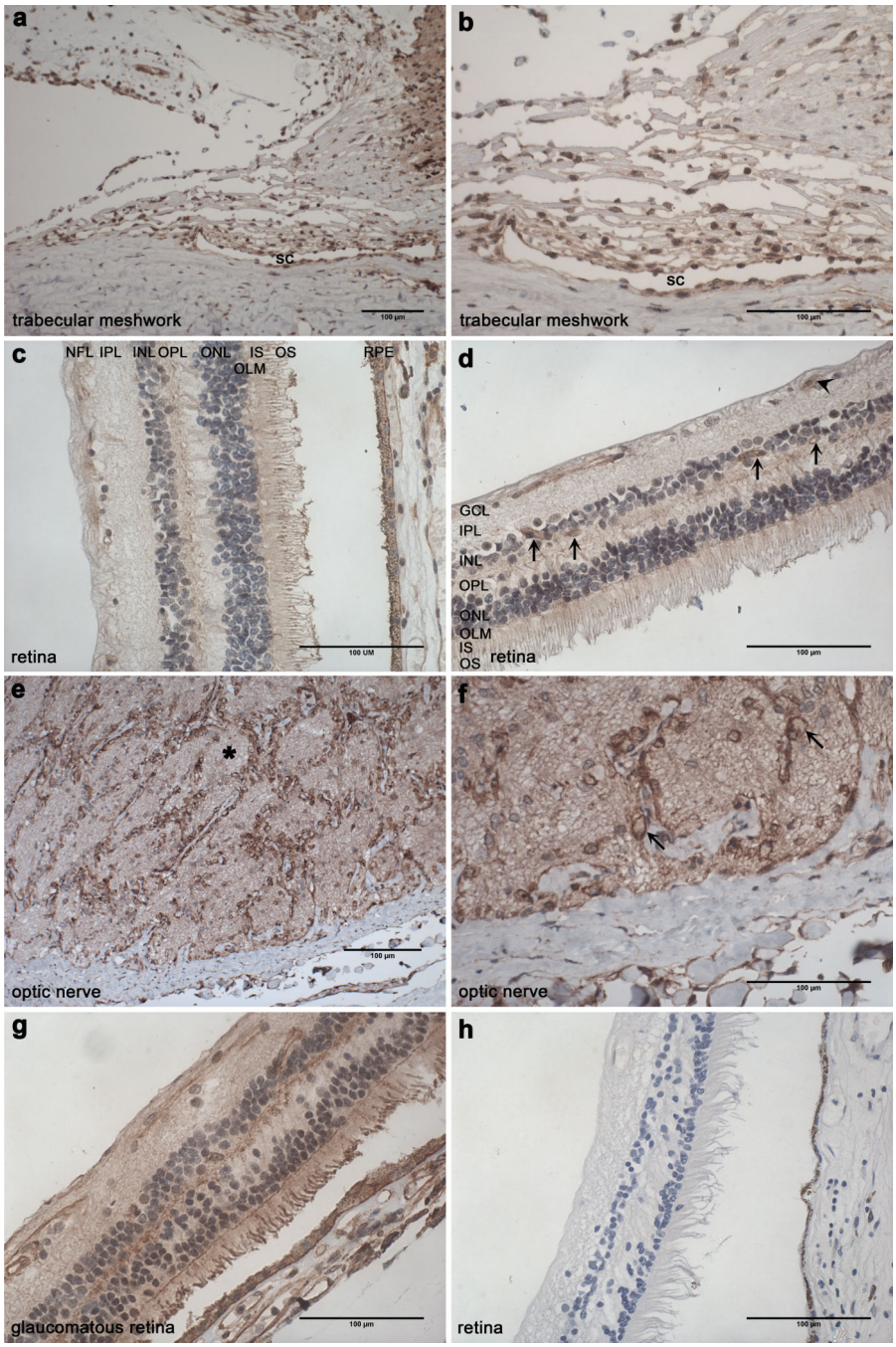

Figure 2. Distribution of the ABCA1 protein in human ocular tissues

Sections of a normal human eye were immunolabelled with the anti-ABCA1 antibody (brown) and counterstained with haemotoxylin to visualise nuclei (blue). Positive immunolabelling was detected in the trabecular meshwork (**a** and **b**), throughout the retina (**c** and **d**) and in the optic nerve (**e** and **f**). In the retina (**c**), comparatively pronounced ABCA1 immunolabelling was observed at the tips of photoreceptors, in the outer limiting membrane (OLM), outer plexiform layer (OPL) and nerve fibre layer (NFL). (**d**) Labelling was also pronounced in some cells in the inner nuclear layer (INL; *arrow*), in retinal

ganglion cells in the ganglion cell layer (GCL; *arrowhead*) and retinal blood vessel wall (not shown). In the optic nerve (**e** and **f**), the protein was distributed in the nerve fibre bundles (**e**, *asterisk*) and at the cell boundary of astrocytes in the glial columns (**f**, *arrow*). In sections of a glaucomatous eye, (data not shown), including in the retina (**g**), similar distribution of the protein to that in the normal eye, was observed. The experiment was repeated for reproducibility. (**h**) Section hybridised with the secondary detection reagent alone as negative control. sc, Schlemm's canal; RPE, retinal pigment epithelium; OS, outer segment; IS, inner segment; ONL, outer nuclear layer; IPL, inner plexiform layer. Scale bar=100μm.

Table 1

Association results for the best SNPs in previously unreported regions with *P*-values < 1×10^{-7} in the discovery cohort.

CHR[a]	SNP	Position[b]	Gene	Risk allele	*P*[c]	OR	SE	Frequency[d]
9	rs2472493	107695848	*ABCA1*[*]	G	2.0×10^{-10}	1.43	0.05	0.51/ 0.43
11	rs11827818	120198728	*ARHGEF12*[*]	G	9.2×10^{-9}	1.52	0.07	0.20/0.14
6	rs114096562	1984385	*GMDS*	A	7.0×10^{-8}	1.55	0.08	0.88/0.83

[a] CHR, chromosome

[b] position in build 37

[c] *P* corrected for genomic inflation factor lambda (λ=1.06)

[d] allele frequency in cases/controls

[*] indicates that the corresponding SNP is not in the indicated gene, instead, characterised gene nearby those SNPs have been shown.

Table 2

Association and meta-analysis of the discovery and replication cohorts for the top ranked loci

Association results for 3 loci which reached genome-wide significance in the discovery cohort, as well as other top ranked loci showing replication. Proxy SNPs are presented where imputed data not available for replication cohorts.

						ANZRAG (discovery)		ANZRAG (replication)		BMES		NEIGHBOR		MEEI		Meta_analysis			
Chr[a]	SNP	Position[b]	A1[c]	A2	Gene	OR	P[d]	OR	P	OR	P[d]	OR	P	OR	P	OR	P	HetISq[e]	HetPVal[f]
3	rs2710323	52815905	T	C	*ITIH1*	1.25	9.16×10^{-5}	1.14	0.005	1.44	0.01	1.06	0.25	0.87	0.31	1.14	4.53×10^{-6}	64.6	0.02
4	rs4619890	7853160	G	A	*AFAP1*	1.26	9.76×10^{-6}	1.20	0.0004	1.07	0.62	1.14	0.008	1.13	0.38	1.20	7.03×10^{-10}	0	0.57
4	rs4478172	7902003	C	A	*AFAP1*	1.29	2.73×10^{-5}	1.15	0.02	1.21	0.26	1.16	0.005	1.11	0.47	1.19	2.19×10^{-8}	0	0.64
6	rs11969985	1922907	G	A	*GMDS*	1.53	3.18×10^{-7}	1.23	0.009	0.92	0.71	1.28	0.001	1.28	0.24	1.31	7.70×10^{-10}	46.4	0.11
6	rs2761233	1949101	T	C	*GMDS*	1.53	3.35×10^{-7}	1.19	0.02	0.94	0.79	1.28	0.001	1.28	0.23	1.29	2.17×10^{-9}	48.5	0.10
9	rs2472493	107695848	G	A	*ABCA1**	1.43	2.08×10^{-10}	1.26	4.84×10^{-6}	1.44	0.01	1.26	7.05×10^{-6}	0.99	0.89	1.31	2.16×10^{-19}	53.6	0.07
11	rs2276035	120346360	A	G	*ARHGEF12*	1.47	1.13×10^{-7}	1.08	0.29	1.05	0.81	1.09	0.15	NA**	NA**	1.18	7.83×10^{-6}	77.1	0.004

[a] Chr, Chromosome

[b] position of SNPS in build 37

[c] effect allele in all the cohorts

[d] *P*-value corrected for genomic inflation factor lambda

[e] I2 statistic which measures heterogeneity on scale 0 to 100%

[f] *P*-values for the heterogeneity test

* indicates that the corresponding SNP is not in the indicated gene/genes, instead, characterised gene/genes nearby those SNPs have been shown

** rs2276035 SNP was not available in MEEI cohort.